

Simulation of the energy spectra of original versus recombined H_2^+ molecular ions transmitted through thin foils

Manuel D. Barriga-Carrasco and Rafael Garcia-Molina

Departamento de Física, Universidad de Murcia, Apartado 4021, E-30080 Murcia, Spain

(Received 24 February 2004; published 9 September 2004)

This work presents the results of computer simulations for the energy spectra of original versus recombined H_2^+ molecular ions transmitted through thin amorphous carbon foils, for a broad range of incident energies. A detailed description of the projectile motion through the target has been done, including nuclear scattering and Coulomb repulsion as well as electronic self-retarding and wake forces; the two latter are calculated in the dielectric formalism framework. Differences in the energy spectra of recombined and original transmitted H_2^+ molecular ions clearly appear in the simulations, in agreement with the available experimental data. Our simulation code also differentiates the contributions due to original and to recombined H_2^+ molecular ions when the energy spectra contain both contributions, a feature that could be used for experimental purposes in estimating the ratio between the number of original and recombined H_2^+ molecular ions transmitted through thin foils.

DOI: 10.1103/PhysRevA.70.032901

PACS number(s): 34.50.Bw, 36.40.-c, 79.20.Rf

I. INTRODUCTION

The interest in the study of H_2^+ molecular ions interacting with thin foils is because H_2^+ is the simplest molecular projectile. It is known that the H_2^+ ion is composed of two protons (separated by a distance R) and a bound electron. When the ion interacts with the foil it travels during a certain time without being dissociated until it loses its bound electron [1], resulting in two protons with a certain space configuration; the elapsed time until it loses its bound electron is called the lifetime of the molecular ion. Sometimes, depending on the initial projectile velocity and on the foil thickness, the molecular ion travels through the foil without being dissociated; this is known as original transmission. The most common thing, at the energies studied in the present work, is that the molecular ion leaves the foil dissociated into the protons that form it, a process called dissociation. But it can happen that the two dissociated protons capture an electron at the exit of the foil [2,3] and recombine to form a H_2^+ ion again; this is said to be recombined to distinguish it from the original transmitted H_2^+ ion.

Original and recombined H_2^+ molecular ions transmitted through thin carbon foils were first identified by Poizat and Remillieux in 1971 [4]. Subsequent measurements of high-energy molecular ion yield versus target thickness by Remillieux and co-workers [2,4–7] and others [8] have demonstrated the existence of two regimes: one corresponding to a rapid decrease of the molecular ion yield with target thickness for very short dwell times, and the other showing a slower decrease of the molecular ion transmission yield for longer dwell times. There is strong evidence that the short dwell time regime represents transmission of the original molecule; for longer dwell times, this transmission probability is negligible, and the detected molecular ions apparently result from recombination of the protons dissociated from the incident H_2^+ molecular ion. Gaillard *et al.* [2] thought that the recombination probability should depend on the probability for electron capture and on the internuclear separation

at the exit surface, which has also been shown in a recent work [3].

The aim of this work is to demonstrate that original and recombined transmitted H_2^+ molecular ions can also be differentiated by their energy losses and not only by their dwell times. For this purpose we simulate in detail the motion through thin carbon foils of H_2^+ molecular ions and their dissociated fragments, in order to obtain the energy spectra of the original and recombined molecular ions at the exit of the target, for a broad range of incident energies.

When the H_2^+ molecular ion arrives at the target, it interacts both with the electrons and with the nuclei of the target. Before dissociating, the H_2^+ ion experiences a stopping force mainly due to the target electrons and a scattering force due to the target nuclei. When it dissociates, its fragments also experience the same forces plus other forces resulting from the close proximity of their partner fragments; namely, they induce a wake electric field in the target electronic medium, affecting the motion of their partners. In addition, when both fragments are charged they mutually repel through Coulomb forces. Finally, in order to take into account the H_2^+ recombination process, we include in the simulations the possibility that the dissociated fragments can capture or lose electrons.

For comparison purposes, in Sec. II we calculate theoretically the electronic stopping of the original and recombined transmitted H_2^+ ions. In Sec. III we present the basic ingredients of our computer calculations, whose results are compared with available experimental data in Sec. IV. The conclusions of this work appear in Sec. V. In what follows we will use atomic units, except where otherwise stated.

II. ELECTRONIC STOPPING OF THE H_2^+ MOLECULAR ION

Energy loss due to electronic excitations in the foil is the main contribution to the stopping of a swift projectile at the energies considered in this work. The interactions of the pro-

jectile with the electrons of the material will be described in the framework of the dielectric formalism, which accounts for the response of the electronic medium to external perturbation through the dielectric function $\epsilon(k, \omega)$, where k and ω are the modulus of the momentum and the energy, respectively, transferred to the electronic excitations of the target.

We use in this work a linear combination of the energy loss function $\text{Im}[-1/\epsilon(k, \omega)]$, for the external electron excitations, which is obtained from the dielectric function proposed by Mermin [9], and a generalized oscillator strength hydrogenlike approach for internal electron excitations [10,11]. With this procedure the optical properties and the energy loss spectra of real materials are properly described for the purposes of swift charged projectile energy loss calculations.

The electronic stopping for a charge density $\rho(\mathbf{r}, t)$ traveling with a constant velocity \mathbf{v} through a solid whose energy loss function is $\text{Im}[-1/\epsilon(k, \omega)]$, is

$$S_e = \frac{2}{\pi v^2} \int_0^\infty \frac{dk}{k} \int_0^{kv} d\omega \omega \rho^2(k) \text{Im} \left[\frac{-1}{\epsilon(k, \omega)} \right], \quad (1)$$

where $\rho(k)$ is the Fourier transform of the projectile charge density.

As the electronic stopping is a statistical process, it is convenient to define the ‘‘straggling,’’ which is the variance of the projectile energy loss per unit path length:

$$\Omega^2 = \frac{2}{\pi v^2} \int_0^\infty \frac{dk}{k} \int_0^{kv} d\omega \omega^2 \rho^2(k) \text{Im} \left[\frac{-1}{\epsilon(k, \omega)} \right]. \quad (2)$$

The charge density of the H_2^+ molecular ion can be written as

$$\rho(\mathbf{r}, t) = Z_1 \delta(\mathbf{r} - \mathbf{v}t - \mathbf{R}/2) + Z_1 \delta(\mathbf{r} - \mathbf{v}t + \mathbf{R}/2) - \rho_{\text{el}}(\mathbf{r} - \mathbf{v}t), \quad (3)$$

where $Z_1=1$ is the charge of the proton, \mathbf{R} is the internuclear vector between protons, \mathbf{v} is the velocity of the H_2^+ projectile, and ρ_{el} is the electronic density of the molecular ion.

We assume in this work that the electronic density ρ_{el} is that of the ground molecular level $\sigma_g 1s$. It is known that the exact electronic wave function of this ground level is an infinite series of Legendre associated functions; the corresponding potential energy has a minimum at $R_{\text{min}} = 1.9972 \text{ a.u.}$ with a value $U(R_{\text{min}}) = -0.6026 \text{ a.u.}$ [12]. But the difficult handling of these functions opens the door to simpler models for the electron wave function of the H_2^+ molecular ion. The Gaussian model [13], which has proved to be simple and useful [14], gives the following wave function:

$$\phi_{\text{el}}(\mathbf{r}) = N_G [\varphi_G(\mathbf{r} - \mathbf{R}/2) + \varphi_G(\mathbf{r} + \mathbf{R}/2)], \quad (4)$$

where $\varphi_G(\mathbf{r})$ is the normalized Gaussian wave function

$$\varphi_G(\mathbf{r}) = \left(\frac{2\alpha}{\pi} \right)^{3/4} \exp(-\alpha r^2), \quad (5)$$

$\alpha = 0.43 \text{ a.u.}$ is the orbital parameter, and N_G is the normalization factor for this molecular orbital:

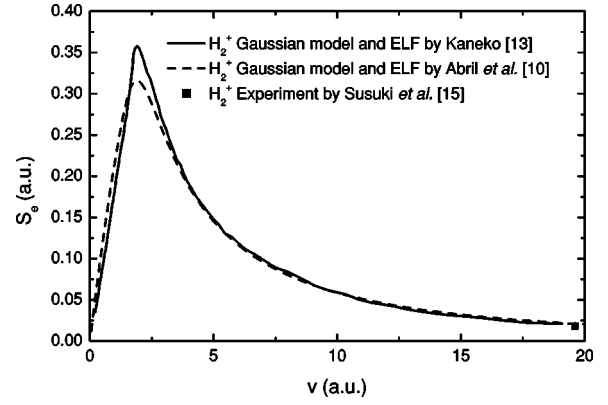


FIG. 1. Electronic stopping of amorphous carbon for H_2^+ , as a function of its velocity. The calculations were done using the Gaussian model with the energy loss function proposed by Kaneko [13] (solid line) and with the energy loss function appearing in Abril *et al.* [10] (dashed line). The symbol \blacksquare represents the experimental result of Susuki *et al.* [15].

$$N_G = \left\{ \frac{1}{2[1 + \exp(-\alpha R^2/2)]} \right\}^{1/2}. \quad (6)$$

The variational method [13] gives $U(R_{\text{min}}) = -0.5031 \text{ a.u.}$ and $R_{\text{min}} = 2.05 \text{ a.u.}$ for the minimum of potential and its corresponding internuclear distance, respectively, both values being quite close to the exact results.

To calculate the stopping power and the straggling for a beam of H_2^+ molecular ions incident with random orientation on the target, we substitute $\rho^2(k)$ in Eqs. (1) and (2) by the square of the Fourier transform of the charge density of the molecular ion and average it for all possible angles between \mathbf{k} and \mathbf{R} , which gives

$$\langle \rho_{\text{ext}}^2(k) \rangle_{\text{ang}} = \mathcal{A}^2(k) \frac{1}{2} \left[1 + \frac{\sin(kR)}{kR} \right] + \mathcal{B}^2(k) - 2\mathcal{A}(k)\mathcal{B}(k) \frac{\sin(kR/2)}{kR/2}, \quad (7)$$

where

$$\mathcal{A}(k) = 2Z_1 - \mathcal{C}(k),$$

$$\mathcal{B}(k) = e^{-\alpha R^2/2} \mathcal{C}(k),$$

and

$$\mathcal{C}(k) = e^{-k^2/8\alpha} / [1 + \exp(-\alpha R^2/2)].$$

We compare in Fig. 1 the electronic stopping of a carbon target for the H_2^+ molecular ion, calculated with our energy loss function [10,11] or with the one used by Kaneko [13], in both cases using a Gaussian model for the electronic molecular orbital. One experimental result is depicted for high velocity ($v = 19.6 \text{ a.u.}$ [15]), i.e., small dwell times, which corresponds to the case of original transmitted molecules.

On the other hand, the energy loss of a recombined H_2^+ molecular ion is similar, except for vicinage effects, to the energy lost by two protons traveling together in an uncorre-

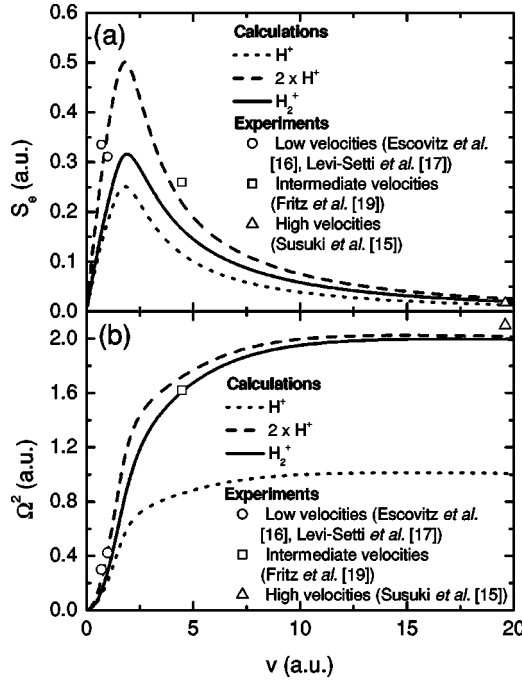


FIG. 2. (a) Electronic stopping and (b) electronic straggling of amorphous carbon for the H_2^+ molecular ion as a function of its velocity, using the Gaussian model (solid line); the corresponding results for H^+ and twice H^+ are represented by dotted and dashed lines, respectively. The symbols represent experimental results [15–17,19] for the different energy regions discussed in detail in Sec. IV.

lated manner, which is twice the energy lost by one proton:

$$\Delta E(H_2^+ \rightarrow H_{2\text{recomb}}^+) \approx 2[\Delta E(H^+ \rightarrow H^+)]. \quad (8)$$

The same holds with the straggling:

$$\Omega^2(H_2^+ \rightarrow H_{2\text{recomb}}^+) \approx 2[\Omega^2(H^+ \rightarrow H^+)]. \quad (9)$$

In Figs. 2(a) and 2(b) we have depicted the electronic stopping and straggling, respectively, obtained here for the original transmitted H_2^+ molecular ion and for twice the corresponding values for a single proton. The calculations for the original transmitted H_2^+ agree with experiments [15] only at high energy, but clearly differ from the available experimental data for the low- [16–18] and intermediate- [19] energy regions. A computer simulation, described in what follows, will help us to understand the behavior of the energy loss of the transmitted H_2^+ in the whole range of incident energies.

III. COMPUTER SIMULATIONS

The numerical code we have used to follow the trajectories of the H_2^+ molecular ions has been described elsewhere [14,20]. Here we summarize its main points.

Inside the target the H_2^+ molecular ion first moves nondissociated and, after a brief time, it breaks into its constituent fragments. The time moving nondissociated is drawn from the lifetime of the H_2^+ molecular ion in carbon, 0.23 fs [15]; during the motion of the molecular ion as a whole its

interactions with the target are different from those that take place when the molecule is dissociated. Nondissociated molecular ions are supposed to experience the same interactions as an atomic projectile [3], suffering (i) the electronic stopping force and (ii) collisions with the target nuclei. The calculation of the electronic stopping force was presented in the previous section; nuclear collisions are taken into account by adapting a Monte Carlo algorithm developed by Möller *et al.* [21] to describe the classical theory of the dispersion using a Thomas-Fermi Coulomb screened potential with a universal screening distance [22,23].

When the incident molecular ion dissociates into its constituent protons, each one is subjected individually to the same types of atomic interactions (i) and (ii), plus other interactions related to the correlated motion of its fragment partner, namely, (iii) the Coulomb repulsion, when both dissociation fragments are charged, and (iv) the wake force, due to the electronic excitations induced in the target by the partner fragment. Coherent scattering is not taken into account because it was shown to represent a small correction in this energy range [24].

The wake force produced by a fragment (with charge density ρ_1) on the other fragment (with charge density ρ_2) at the relative position given by the cylindrical coordinates (z, r) is calculated using the same dielectric formalism as for the stopping force [14]. The components of this force parallel and perpendicular to the motion of a fragment with charge density ρ_1 are

$$F_z(z, r) = \frac{2}{\pi v^2} \int_0^\infty dk \frac{\rho_1(k)\rho_2(k)}{k} \int_0^{kv} d\omega \omega J_0(r\sqrt{k^2 - \omega^2/v^2}) \times \left\{ \sin\left(\frac{\omega z}{v}\right) \text{Re}\left[\frac{1}{\epsilon(k, \omega)} - 1\right] + \cos\left(\frac{\omega z}{v}\right) \text{Im}\left[\frac{1}{\epsilon(k, \omega)} - 1\right] \right\} \quad (10)$$

and

$$F_r(z, r) = \frac{2}{\pi v} \int_0^\infty dk \frac{\rho_1(k)\rho_2(k)}{k} \int_0^{kv} d\omega \sqrt{k^2 - \omega^2/v^2} \times J_1(r\sqrt{k^2 - \omega^2/v^2}) \times \left\{ \cos\left(\frac{\omega z}{v}\right) \text{Re}\left[\frac{1}{\epsilon(k, \omega)} - 1\right] - \sin\left(\frac{\omega z}{v}\right) \text{Im}\left[\frac{1}{\epsilon(k, \omega)} - 1\right] \right\}, \quad (11)$$

where $J_0(\dots)$ and $J_1(\dots)$ are Bessel functions of the first kind.

The initial geometry of the incident H_2^+ molecular ion must be taken into account because the forces between fragments depend on the internuclear distance as well as on the orientation of the internuclear axis with respect to the beam direction. The initial internuclear distance is taken from a distribution theoretically calculated using the Franck-Condon principle [25]; the initial molecular orientation is obtained from a random draw of Euler angles [26].

The simulation code uses a standard molecular dynamics method to follow the evolution of a system of one (the non-

dissociated molecular ion) or several particles (i.e., the fragments), using a numerical integration of Newton equations. The possibility that the fragments can capture or lose an electron inside the foil is also considered in a simple way, in order to account for the recombination process. The H^- fraction is negligible in the energy range studied here [27,28] and so only H^+ and H^0 fragments will be considered:

$$\rho(k) = \begin{cases} 1 & \text{for } H^+, \\ 1 - \frac{1}{[1 + (k/2)^2]^2} & \text{for } H^0. \end{cases} \quad (12)$$

To implement the electron capture or loss process in the computer code, the charge state of each fragment has been assigned at each time step according to the equilibrium charge fraction corresponding to its velocity [27,28]. Nuclear collisions suffered by the dissociated fragments are insensible to their charge state, behaving like protons for these types of collisions. The stopping force acting on a fragment depends on its charge state, but the wake force depends on the charge state of both interacting fragments. Finally, Coulomb repulsion takes place only when both fragments are protons; this interaction is also considered outside the foil because repulsion inside the target is not complete, especially at the highest fragment velocities. The trajectories are calculated until each projectile reaches a simulated detector, characterized by an angular acceptance that takes into account the effects of finite resolution.

The computer code also considers that, once the fragments reach the exit surface of the foil, molecular recombination can take place only when one electron is captured by one of the two fragment protons, and the system (two protons and the captured electron) forms a bound state of the H_2^+ molecular ion. In order for the system to be bound, its internal energy should be smaller than the maximum of the ion effective potential energy for dissociation, i.e.,

$$E_{\text{int}} < U_{\text{eff max}}(R, v_{\text{rel}}) \Rightarrow \text{recombination}, \quad (13)$$

$$E_{\text{int}} > U_{\text{eff max}}(R, v_{\text{rel}}) \Rightarrow \text{no recombination}. \quad (14)$$

In this work, we consider that the recombination happens only for the $\sigma_g 1s$ electronic state (or fundamental electronic state of the H_2^+ molecular ion) so the effective potential energy will correspond to this fundamental state. The internal energy of the system is given by the relative kinetic energy and the H_2^+ dissociation effective potential energy for the $\sigma_g 1s$ electronic state, U_{eff} , which depends on the distance R and on the relative velocity v_{rel} between the two protons:

$$E_{\text{int}} = \frac{1}{2}\mu v_{\text{rel}}^2 + U_{\text{eff}}(R, v_{\text{rel}}) = \frac{1}{2}\mu v_{\text{rel}}^2 + U(R) + \frac{L^2}{2\mu R^2}, \quad (15)$$

where $U(R)$ is the H_2^+ dissociation potential from [29], μ is the reduced mass of the system, and $\mathbf{L} = \mu \mathbf{R} \times \mathbf{v}_{\text{rel}}$ is the relative angular momentum of the system. Also, the value of the internuclear distance R must be comprised between the values of the classic turning points of the effective potential well U_{eff} .

To recombine the H_2^+ ion in our simulation code, first of all we need the particles that form the H_2^+ ion: the two protons and the electron. The latter is captured from the electronic medium of the target material taking into account the possibility of a two-individual-proton electronic capture. We have considered this capture at the exit surface of the foil also, as this is more probable since the electron attraction by the two protons is not screened by the material electrons. Our code allows us to know the coordinates and the velocity of each dissociated proton at any instant, and therefore we can know the relative magnitudes \mathbf{R} , \mathbf{v}_{rel} , and \mathbf{L} at the exit of the foil. Knowing these values, it is possible to calculate the internal energy as well as the maximum of the dissociation effective potential energy in order to decide if the H_2^+ recombination happens.

IV. RESULTS

The energy spectra of the H_2^+ molecular ions transmitted through amorphous carbon foils were obtained using the previously described code, and they will be compared with the available experimental data according to the H_2^+ incident energies: low [16–18], intermediate [19], and high energies [15].

A. Low energies

The experiments performed in Refs. [16–18] studied the transit of H_2^+ molecular ions with $v \leq 1.00$ a.u. (≤ 50 keV). At these low incident velocities, very thin foils were needed to detect original transmitted H_2^+ molecular ions. Also at these velocities, the number of transmitted H_2^+ molecular ions formed after recombination is very high, because the probability that the proton fragments capture an electron and become a hydrogen atom is also high ($\approx 70\%$), and molecular recombination depends directly on this electron capture by the exiting proton fragments [3].

Figure 3 shows simulated and experimental energy distributions for different incident H_2^+ velocities and for different foil thicknesses. Our code can distinguish between the energy spectra of the original and recombined transmitted H_2^+ molecular ions. It can be seen that almost all the H_2^+ ions experimentally detected are recombined ones. The number of recombined and original molecular ions decreases with increasing dwell time, but the recombination process dominates for larger dwell times (i.e., low energies) [3]. Recombined molecular ions are characterized by a mean energy loss and a width in the energy distribution that is larger than that for the original transmitted ones, as is expected according to the discussion in Sec. II.

Moreover, it can be seen that the number of recombined molecular ions is independent of the dissociated fragment energy before they recombine, as all energy distributions are practically symmetric around a mean value. The small asymmetry at low spectrum energies is due to particles that suffer few nuclear collisions during their travel through the foil; this is demonstrated when this asymmetry disappears as the energy of the incident particle increases. This feature is more remarkable for the experimental distributions. The sums of

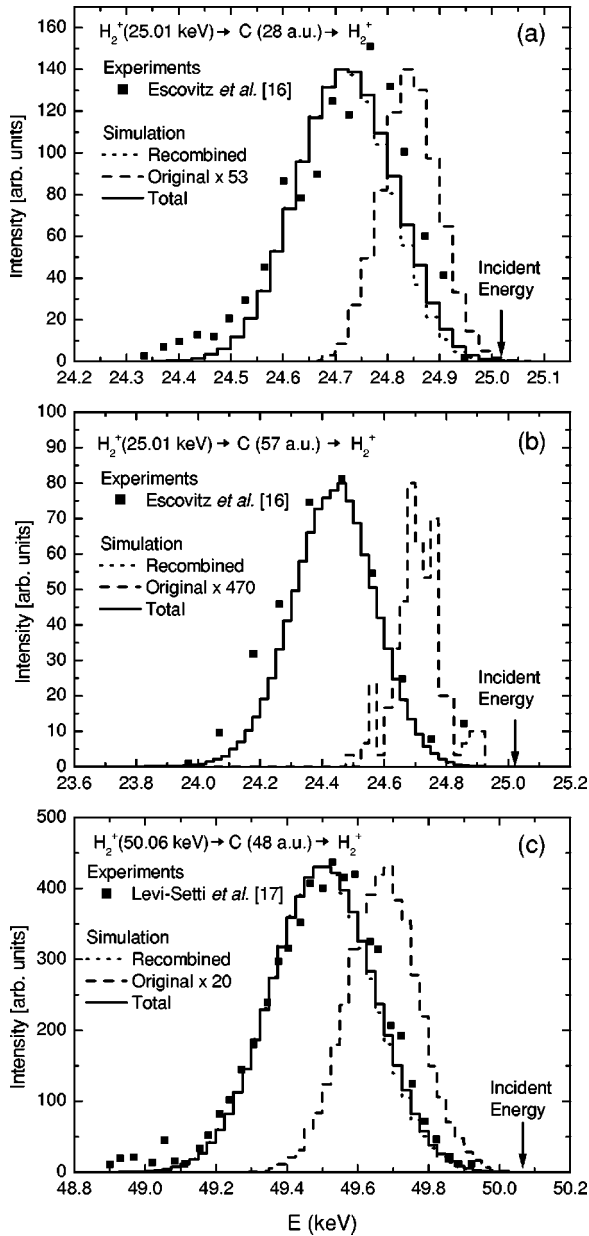


FIG. 3. Energy distributions of H_2^+ molecular ions transmitted through amorphous carbon foils and detected at all angles, for different incident energies (E) and target thicknesses (D). (a) $E = 25.01$ keV, $D = 28$ a.u., (b) $E = 25.01$ keV, $D = 57$ a.u., and (c) $E = 50.06$ keV, $D = 48$ a.u. Simulated spectra for transmitted H_2^+ molecular ions after recombination (dotted line), original ones [dashed lines, enlarged (a) 53, (b) 470, and (c) 20 times] and the sum of both (solid line) are compared with experimental results [16,17]. Note that in (b) the dotted line is hidden beneath the solid one.

the simulated energy distributions for the original and recombined molecular ions are depicted by continuous lines in Fig. 3 and agree quite well with the distributions obtained experimentally.

Also, from the spectra shown in Fig. 3 we can obtain the experimental stopping and straggling, which can be compared with our calculations in Sec. II. The experimental stopping is the difference between the incident energy and the mean value of the energy distribution, divided by the foil

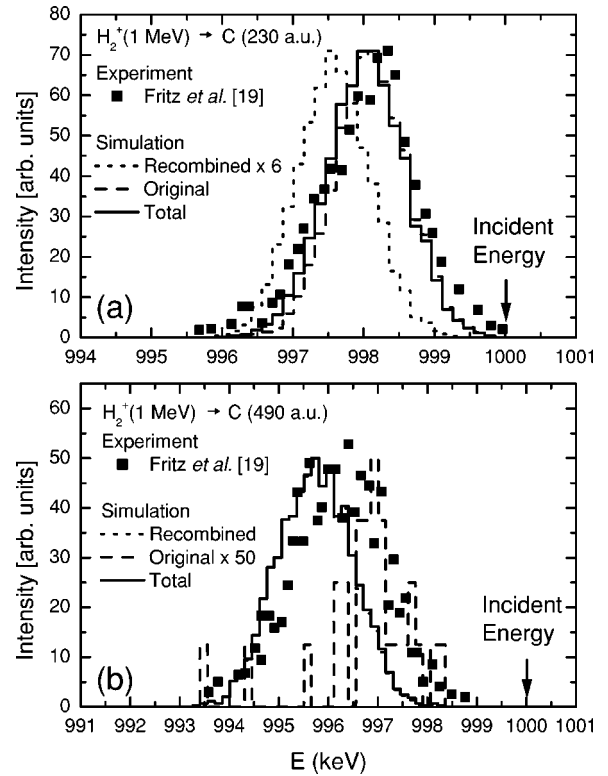


FIG. 4. Energy spectra of H_2^+ molecular ions transmitted through amorphous carbon foils of thickness (a) 230 and (b) 490 a.u. The incident beam energy is 1 MeV ($v = 4.47$ a.u.). Our simulations are compared with experimental results by Fritz *et al.* [19]; recombined ions [dotted line, (a) enlarged six times], original ions [dashed line, (b) enlarged 50 times], and total ions (solid line). In (b), the dotted line practically coincides with the solid one.

thickness (D). The straggling is related to the square of the full width at half maximum of the energy distribution through

$$\Omega^2 = \frac{N_{FWHM}^2}{D\sqrt{8 \ln 2}}. \quad (16)$$

The values $S_e = 0.34 \pm 0.01$ a.u. and $\Omega^2 = 0.30 \pm 0.01$ a.u. are obtained from Figs. 3(a) and 3(b); whereas $S_e = 0.31 \pm 0.01$ a.u. and $\Omega^2 = 0.43 \pm 0.01$ a.u. result from Fig. 3(c). If these values are put on the theoretical Fig. 2, it is noticed that these data are more similar to twice the proton values (characteristic of a recombination process) than to the H_2^+ theoretical values (characteristic of an original transmission). This means that in these experiments most of the transmitted H_2^+ molecular ions result from recombination of their fragments.

B. Intermediate energies

In the experiment by Fritz *et al.* [19], 1 MeV H_2^+ molecular ions ($v = 4.47$ a.u.) were sent through amorphous carbon foils with thicknesses in the range of 230 a.u. to 920 a.u. Figures 4(a) and 4(b) represent the final H_2^+ energy distributions for the 230- a.u.- and 490- a.u.-thick foils, respectively, and clearly show how the spectra widen for the thicker tar-

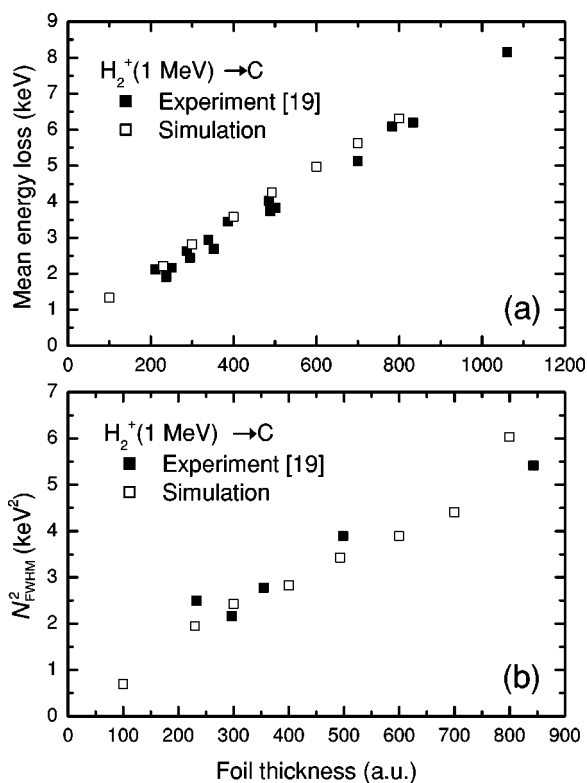


FIG. 5. (a) Mean value and (b) N_{FWHM}^2 of the energy lost by H_2^+ molecular ions transmitted through amorphous carbon foils, as a function of the foil thickness, for an incident 1 MeV H_2^+ molecular ion beam. The experimental data by Fritz *et al.* [19] are shown by ■; the results obtained from our simulations of the energy distributions are represented by □.

get. Our simulations agree quite well with the experimental distributions.

For the thinner foil, Fig. 4(a), the number of original transmitted ions is greater than the number of recombined ones, because the shorter dwell times favor the transmission of original H_2^+ molecular ions, and, in addition, the neutral fragment fraction (0.3%) [30] after H_2^+ dissociation is much smaller at these energies than at low energies. On the other hand, for the thicker foil, Fig. 4(b), fewer original ions are transmitted and so the recombined yield is greater than the original one.

It is possible to obtain the mean energy loss as the difference between the incident energy and the mean energy of the energy distributions. In this way the mean energy loss for several foil thicknesses between 100 and 1100 a.u. has been calculated and represented in Fig. 5(a) together with the experimental results [19], showing an excellent agreement. The mean energy loss increases linearly with the foil thickness, the slope being $S_e = 0.260 \pm 0.006$ a.u. Putting this stopping value in Fig. 2(a), we see that it is rather close to twice the H^+ stopping at the same velocity.

The energy straggling of the transmitted H_2^+ molecular ions can also be obtained from the energy distributions. Figure 5(b) represents the square of the full width at half maximum (N_{FWHM}^2) as a function of foil thickness. As in Fig. 5(a), our calculations compare quite well with experimental re-

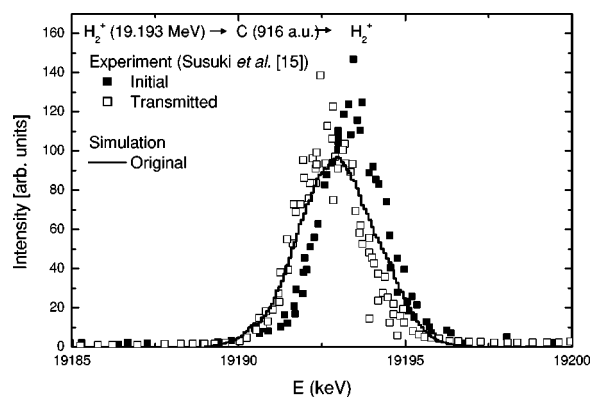


FIG. 6. Energy distribution of H_2^+ transmitted through a 916-a.u.-thick amorphous carbon foil, for an incident beam energy of 19.193 MeV ($v=19.6$ a.u.). The energy distribution of transmitted molecular ions obtained with our program (histogram) is compared with experimental results (□) [15]; the experimental energy distribution of the incident beam (without the foil) is represented by ■ [15].

sults [19]. N_{FWHM}^2 grows linearly with the foil thickness, obtaining the straggling value $\Omega^2 = 1.5 \pm 0.4$ a.u. If this value is put in Fig. 2(b), it is seen that its error bar includes the value of twice the proton straggling. The value of N_{FWHM}^2 at zero thickness agrees with the experimental width of the initial beam energy distribution, $N_{FWHM}^2 \phi = 1.3 \pm 0.7$ a.u. [19].

All together, our results lead us to conclude that for intermediate energies the recombination mechanism is the main process for thick foils, while the original transmission is the main process for thin foils.

C. High energies

Finally, we discuss the experiment of Susuki *et al.* [15], where the energy loss of 19.2 MeV H_2^+ molecular ions ($v=19.6$ a.u.) was measured at the exit of amorphous carbon foils with thicknesses ranging from 170 a.u. to 970 a.u.

As was mentioned before, our simulation program differentiates between original and recombined transmitted molecular ions, so it is possible to say if the experimentally detected ions are mostly originals or recombined ones just by analyzing the energy loss distributions. As an example, Fig. 6 shows the experimental and simulated energy distributions of H_2^+ molecular ions transmitted through a 916-a.u.-thick amorphous carbon foil. Recombined molecular ions are not obtained in the simulation for this energy and for this foil thickness, which means that the experimentally detected molecular ions were overall original ones. The energy distribution of the incident beam is also shown in Fig. 6 for comparison purposes.

The stopping power is calculated from the experimental energy distribution in the same way as for low and intermediate energies, obtaining $S_e = 1.81 \pm 0.15 \times 10^{-2}$ a.u. Putting this result in Fig. 2(a), we notice that this value is closer to the electronic stopping power for H_2^+ than to twice the electronic stopping power for a proton, just as would correspond to an original transmission process.

The value for the straggling obtained from the same experimental energy distribution is $\Omega^2 = 2.1 \pm 0.3$ a.u., which is slightly larger than the theoretical result for the H_2^+ molecular ion [Fig. 2(b)]; this is so because the energy distribution of the incident beam already has a considerable width, $N_{\text{FWHM}}^2 = 56.64 \pm 0.03 \times 10^3$ a.u., as Fig. 6 shows.

When depicting the energy loss spectra for the same incident energies but for different target thicknesses, it is seen that the thicker is the foil (i.e., for longer dwell times) the smaller is the detected number of original H_2^+ molecular ions relative to the number of recombined ones. This is due to the finite lifetime in the foil of the molecular ion; therefore for longer dwell times fewer original molecular ions are transmitted. But we do not obtain the same ratio for different incident energies with similar dwell times (~ 1 fs) as in Figs. 3(a), 3(c), 4(a), and 6. At first glance, the ratio between the number of original transmitted molecular ions and the number of recombined ones increases with incident energy. This could be due to a dependence of the lifetime on the energy, but we have demonstrated recently [3] that it is the recombination yield that really depends on the energy, as electron capture diminishes with increasing energy.

V. CONCLUSIONS

The energy spectra of H_2^+ molecular ions transmitted through thin carbon foils, as a function of the incident projectile energy and target thickness, have been simulated using a computer code that takes into account the main interactions experienced by the molecular ion and its dissociated fragments as they move through the solid. The electronic stopping for these ions was calculated theoretically using the dielectric formalism with an energy loss function that properly describes the electronic excitations of the target material, obtaining the result that the electronic stopping for the H_2^+ molecular ion is smaller than twice the electronic stopping of an isotachic proton.

Two types of transmitted H_2^+ molecular ions have been analyzed: original and recombined ones. To distinguish them, we have implemented in our simulation code the motion through the solid of the initially nondissociated H_2^+ molecu-

lar ion during a short time and, after the dissociation takes place, the correlated motion of each pair of its dissociated fragments. We have considered that the projectiles experience the following interactions: stopping force, nuclear scattering, wake force, and Coulomb explosion, the two latter appearing only for the dissociated fragments. The possibility of electron capture or loss by these fragments has also been included in our simulation in order to consider the recombination of H_2^+ molecular ions. The simulated energy spectra for original and recombined transmitted H_2^+ molecular ions compare quite well with the experimental spectra.

In a previous paper [3] we discussed the transmission of original or recombined H_2^+ molecular ions according to their dwell times in the foil. The results shown in the present work show that the original and recombined transmitted H_2^+ molecular ions can also be distinguished by comparing their energy loss characteristics, derived from their energy spectra, with the energy loss calculations obtained within the dielectric formalism framework. The energy loss of an original transmitted H_2^+ molecular ion is similar to the calculated electronic energy loss of the H_2^+ molecular ion, while the energy loss of a recombined H_2^+ molecular ion is similar to twice the calculated energy loss of a proton. The same happens for the energy straggling; the energy straggling of the original transmitted molecular ion is similar to the calculated H_2^+ electronic energy straggling, while the energy straggling of the recombined molecular ion is similar to twice the proton electronic energy straggling.

In conclusion, the computer code that we have developed reproduces satisfactorily the main features that appear in the dissociation, recombination, and transmission of H_2^+ molecular ions through thin carbon foils.

ACKNOWLEDGMENTS

This work was financed by the Spanish Ministerio de Ciencia y Tecnología (through Project No. BFM2003-04457-C02-01) and the Spanish Ministerio de Educación, Cultura y Deporte (M.D.B-C.). M.D.B-C. thanks the Fundación Séneca for partial financial support and J. Barriga for fruitful discussions.

-
- [1] N. Bohr, K. Dan. Vidensk. Selsk. Mat. Fys. Medd. **18**, No. 8 (1948).
 - [2] M. J. Gaillard, J. C. Poizat, A. Ratkowski, and J. Remillieux, Nucl. Instrum. Methods **132**, 69 (1976).
 - [3] R. Garcia-Molina and M. D. Barriga-Carrasco, Phys. Rev. A **68**, 054901 (2003).
 - [4] J. C. Poizat and J. Remillieux, Phys. Lett. **34A**, 53 (1971).
 - [5] N. Cue, N. V. de Castro Faria, M. J. Gaillard, J. C. Poizat, and J. Remillieux, Nucl. Instrum. Methods **170**, 67 (1980).
 - [6] N. Cue, N. V. de Castro-Faria, M. J. Gaillard, J. C. Poizat, J. Remillieux, D. S. Gemmell, and I. Plessner, Phys. Rev. Lett. **45**, 613 (1980).
 - [7] J. Remillieux, Nucl. Instrum. Methods **170**, 31 (1980).
 - [8] W. Brandt, R. Laubert, and A. Ratkowski, Nucl. Instrum. Methods **132**, 57 (1976).
 - [9] N. D. Mermin, Phys. Rev. B **1**, 2362 (1970).
 - [10] I. Abril, R. Garcia-Molina, C. D. Denton, F. J. Pérez-Pérez, and N. R. Arista, Phys. Rev. A **58**, 357 (1998).
 - [11] J. C. Moreno-Marín, I. Abril, and R. Garcia-Molina, Nucl. Instrum. Methods Phys. Res. B **193**, 30 (2002).
 - [12] I. N. Levine, *Quantum Chemistry* (Prentice-Hall, Englewood Cliffs, NJ, 1991).
 - [13] T. Kaneko, Phys. Rev. A **51**, 535 (1995).
 - [14] M. D. Barriga-Carrasco and R. Garcia-Molina, Phys. Rev. A **68**, 062902 (2003).
 - [15] Y. Susuki, M. Fritz, K. Kimura, M. Mannami, N. Sakamoto, H. Ogawa, I. Katayama, T. Noro, and H. Ikegami, Phys. Rev. A **50**, 3533 (1994).

- [16] W. H. Escovitz, T. R. Fox, and R. Levi-Setti, IEEE Trans. Nucl. Sci. **NS-26**, 1147 (1979).
- [17] R. Levi-Setti, K. Lam, and T. R. Fox, Nucl. Instrum. Methods Phys. Res. **194**, 281 (1982).
- [18] T. R. Fox, K. Lam, and R. Levi-Setti, Nucl. Instrum. Methods Phys. Res. **194**, 285 (1982).
- [19] M. Fritz, K. Kimura, Y. Susuki, and M. Mannami, Phys. Rev. A **50**, 2405 (1994).
- [20] R. Garcia-Molina, C. D. Denton, I. Abril, and N. R. Arista, Phys. Rev. A **62**, 012901 (2000).
- [21] W. Möller, G. Pospiech, and G. Schrieder, Nucl. Instrum. Methods **130**, 265 (1975).
- [22] J. F. Ziegler, J. P. Biersack, and U. Littmark, *The Stopping and Range of Ions in Solids*, The Stopping and Ranges of Ions in Matter Vol. 1 (Pergamon, New York, 1985).
- [23] M. Nastasi, J. W. Mayer, and J. K. Hirvonen, *Ion-Solid Interactions: Fundamentals and Applications* (Cambridge University Press, Cambridge, England, 1996).
- [24] R. Garcia-Molina, I. Abril, C. D. Denton, and N. R. Arista, Nucl. Instrum. Methods Phys. Res. B **164–165**, 310 (2000).
- [25] W. L. Walters, D. G. Costello, J. G. Skofronick, D. W. Palmer, W. E. Kane, and R. G. Herb, Phys. Rev. **125**, 2012 (1962).
- [26] M. D. Barriga-Carrasco, Ph.D. thesis, Universidad de Murcia, 2002.
- [27] S. Kreussler and R. Sizmman, Phys. Rev. B **26**, 520 (1982).
- [28] N. V. de Castro Faria, F. L. Freire, Jr., J. M. F. Jeronymo, E. C. Montenegro, A. G. de Pinho, and D. P. Almeida, Nucl. Instrum. Methods Phys. Res. B **17**, 321 (1986).
- [29] A. Aguado, O. Roncero, C. Tablero, C. Sanz, and M. Paniagua, J. Chem. Phys. **112**, 1240 (2000).
- [30] I. Abril, C. D. Denton, M. D. Barriga-Carrasco, R. Garcia-Molina, K. Kimura, and N. R. Arista, Phys. Status Solidi (to be published).